

Performance evaluation of unmanned aerial vehicle wing made from sterculiasetigeradelile fiber and pterocarpuserinaceus wood dust epoxy composite using finite element method Abaqus and structural testing

Nasir Mohammed Tahir, Adamu Umar Alhaji, Ibrahim Abdullahi

Online Publication Date: 20 July 2022

URL: <http://www.jresm.org/archive/resm2022.378ma0102tn.html>

DOI: <http://dx.doi.org/10.17515/resm2022.378ma0102tn>

Journal Abbreviation: *Res. Eng. Struct. Mater.*

To cite this article

Tahşr NM, Alhaji AU, Abdullahi I. Performance evaluation of unmanned aerial vehicle wing made from sterculiasetigeradelile fiber and pterocarpuserinaceus wood dust epoxy composite using finite element method Abaqus and structural testing. *Res. Eng. Struct. Mater.*, 2022; 8(4): 675-694.

Disclaimer

All the opinions and statements expressed in the papers are on the responsibility of author(s) and are not to be regarded as those of the journal of Research on Engineering Structures and Materials (RESM) organization or related parties. The publishers make no warranty, explicit or implied, or make any representation with respect to the contents of any article will be complete or accurate or up to date. The accuracy of any instructions, equations, or other information should be independently verified. The publisher and related parties shall not be liable for any loss, actions, claims, proceedings, demand or costs or damages whatsoever or howsoever caused arising directly or indirectly in connection with use of the information given in the journal or related means.



Published articles are freely available to users under the terms of Creative Commons Attribution - NonCommercial 4.0 International Public License, as currently displayed at [here](https://creativecommons.org/licenses/by-nc/4.0/) (the "CC BY - NC").



Technical Note

Performance evaluation of unmanned aerial vehicle wing made from *sterculiasetigeradelile* fiber and *pterocarpuserinaceus* wood dust epoxy composite using finite element method Abaqus and structural testing

Nasir Mohammed Tahir^{*1,a}, Adamu Umar Alhaji^{2,b}, Ibrahim Abdullahi^{2,c}

¹National Space Research and Development Agency

²Department of Mechanical Engineering, Bayero University, Kano

Article Info

Abstract

Article history:

Received 02 Jan 2022

Revised 06 Jul 2022

Accepted 18 Jul 2022

Keywords:

Unmanned Aerial Vehicle Wing (UAV);
Finite Element Method;
Abaqus Software;
Schrenk Method;
Sterculiasetigeradelile fiber (SSD);
Pterocarpuserinaceus (PTE) wood dust;
Structural Testing.

Finite Element Method such as Abaqus software is increasingly used to analyze structures such as the Unmanned Aerial Vehicle Wing. Unmanned Aerial Vehicle is usually fabricated using synthetic materials such as Glass fibers, Carbon fibers and Kevlar. The problems with the synthetic fibers are environmental pollution during processing, energy consumption during processing and cost of production. Natural fibres can be used as replacement for synthetic fibers due to their comparable physical and mechanical properties. The research involves the simulation of an Unmanned Aerial Vehicle wing made from 5% Cold Alkaline treated 5% *Sterculiasetigeradelile* fiber (SSD) at 0-degree orientation and 7.5% *Pterocarpuserinaceus* (PTE) Wood dust Epoxy composite using Abaqus software. The wing was subjected to aerodynamic wing loading from 167.57N to 895N (3kg to 16kg). The result showed that the wing produced using the Novel material could withstand the most critical flight load distribution in conformation with Federal Aviation Regulation (FAR) part 23 Airworthiness standards with an ultimate design load of 5.7. At the point of failure, the wing could withstand an Ultimate load factor of 20.26. Structural physical testing was performed for a wing loading of 167.75N to 335.50N (3kg to 6kg). The wing successfully resisted the critical in-flight loading confirming the simulation result. The Novel material of lower density (1.093g/cm³) could withstand the wing loading requirement making it suitable for the UAV wing application.

© 2022 MIM Research Group. All rights reserved.

1. Introduction

Unmanned Aerial Vehicles (UAVs) have been used with great success for military intelligence providing an alternative to manned craft due to their small size, reduced risk of life and reduced cost. The Vehicles have many civil applications which include search and rescue missions, exploration, surveying of oil pipelines, forest fires and agricultural applications [1]. Unmanned Aerial Vehicle wings are in airfoil shape and are designed to develop lift when they are moved through the air. Unmanned Aerial Vehicles are commonly produced using synthetic fibres such as Carbon fiber and Glass fiber. The problems with synthetic fibers include high energy consumption during processing, environmental pollution and high cost. Natural fibres such as the *Sterculiasetigeradelile* fibre have not been explored for Unmanned Aerial Vehicles but have the mechanical and physical properties that could withstand the aerodynamic loading requirements. In 1940, spitfire fuselage was designed and built using flax fibres reinforced in phenolic resin. The material was stacked together at different orientations and then hot pressed. The material was known by the name Aerolite. The material was used for the main spar of the Bristol Breinheim bomber [2].

*Corresponding author: n-tahir@hotmail.co.uk

^a orcid.org/0000-0003-0553-3968; ^b orcid.org/0000-0002-0738-4129; ^c orcid.org/0000-0002-9555-3630;
DOI: <http://dx.doi.org/10.17515/resm2022.378ma0102tn>

The finite element method (FEM) is the numerical method used to solve the boundary value problem. The finite element method involves the representation of a given domain as a collection of discrete parts. The essence of the finite element method is to divide the original continuum of the complicated geometry with infinite numbers of the degree of freedom (DOF) into several subdivisions of the continuum with specific geometry termed elements. The elements are interconnected at specific points on the sides of the elements. These are called nodes in the discretized model. Element equations are derived for each of the elements in the discretized model based on appropriate physical theories and principles [3].

Numerical analysis was conducted in predicting the response of structures to given load. i.e the lift distributed along the wing span following the Schrenk method lift distribution calculation. The numerical method was conducted for half wing span in order to reduce the computation time due to symmetry of the UAV wing. The desired output was to find whether the UAV wing could withstand the given load [4]. The model of the UAV wing was developed using ABAQUS/CAE Version 6.11 FE analysis commercial software.

An optimized composite material from 5% Cold Alkaline treated 5% SterculiaSetigeraDelile fibre (SSD) at 0-degree orientation and 7.5% PterocarpusErinaceus (PTE) Wood dust Epoxy have been produced for the potential application. This research involves the simulation of an Unmanned Aerial Vehicle wing using wood fiber and wood dust reinforcements using Abaqus software and Structural testing was used to validate the model.

Synthetic fibres such as Carbon fibre, Glass fibre and Epoxy Matrix are commonly used for the production of Aerospace structures but the production of the fibres has negative impact on the environment. The work is novel in the fact that a new material was made from wood fibre, wood dust and epoxy matrix was used in the production of the Unmanned Aerial Vehicle wing. The wing produced can withstand the critical flight load distribution in conformation with Federal Aviation Regulation. The Novel material could be used as a potential replacement for Carbon fibres in some aerospace applications.

Sullivan, Hwang, Rais-Rohani and Lacy (2009) investigated the strength and stiffness characteristics of a carbon composite wing of an ultralight unmanned Aerial Vehicle. The wing consisted of a foam-core sandwich skin and multiple spars with varying laminate ply pattern and wall thickness dimension. A three-tier whiffle tree was designed for the structural testing of the UAV wing and was used to subject the wing to load in a manner that was consistent with a pull-over-maneuver condition. The wing was loaded incrementally beyond the limit load and the design ultimate load to the point of structural failure. Abaqus software was used to develop the finite element model of the wing; boundary conditions were applied. The static response under simulated wing loading condition was obtained. The strain and deflection prediction from the finite element method were found to be in good agreement with the experimental observation. Despite the Carbon fibre being light, the UAV wing was found to be strong with strength to weight ratio of at least 40 at failure. The Ultralight UAV structural components were designed using Federal Aviation Regulation (FAR) Part 23(normal category) airworthiness standard. The forces applied at each loading condition for the limit load condition of 3.8g and an Ultimate load condition of 5.7g. At the point of failure, the strength to weight ratio was 40 times greater. The result obtained at the point of failure was 17% higher than the Ultimate design load factor [5].

Rumayshah, Prayoga and Moelyadi (2018) designed High Altitude long endurance UAV. Structural testing of composite wing was performed using Finite Element Method. ABAQUS/CAE was used to predict the stress and the deformation of the wing when subjected to loading. The UAV was initially produced using Balsa wood and failed during

flight test as a result of extreme side wind leading to extreme bending. A second generation UAV was designed using composite materials for the wing structure. For the second generation HALE UAV ITB, the UAV had a wing span of 16m, with a chord length of 0.4m. The CAD model was first generated using CATIA V5 in 3D. The part was translated into ABAQUS/CAE. The material used for the UAV was Woven Carbon Epoxy at different fibre orientation and stacking sequence. Non-linear Prandtl Lifting Line Theory (NLLT) was used to estimate the lift distribution on the UAV wing. The weight of the UAV wing was automatically processed considering the material density input in the Abaqus preprocessing. ENCASTE boundary condition was applied to the wing root rib to prevent translation and rotations in all directions. The wing tip was free from all constraints. The overall load and boundary condition are applied to the UAV wing. The global seed was generated for the whole model with a size of approximately 5mm. The total displacement was 3.265m. The new structural configuration had a Tsai-Wu failure criterion is at a value of 0.865[4].

Kanesun, Mansor and Abdul-latif (2014) performed structural and finite element analysis on UAV wing. The geometrical modeling of the wing structural components was conducted in Solidworks and imported into Abaqus/CAE. Only half of the wing was modeled to reduce the total number of elements used in the analysis. The wing skin was made from Carbon fibre fabric, Kevlar Veil and Honey comb cores. The experiment was conducted on the UAV full wing provided by Unmanned System Technology Sdn Bhd. Sandbags weighing 1kg was used to represent the aerodynamic loads on the wing. The deflection values between the bending values and finite element analysis using Abaqus was between ranges 0.35% to 16.4%. The span length(b) 5.1257m, chord length, 0.5886m, mass 45.5kg, number of spar 2 and number of ribs 12[6].

Hutagalung, Latif and Israr (2016) performed structural analysis on a composite UAV wing using Abaqus FEM simulation software. The semi-monoque structure consists of one main mono-spar, 4 major ribs, carbon tubes and a flap. The CAMAR UAV wing was designed using solidwork 2014. The internal components consisted of monospar, 5 leading edge ribs, 5 trailing edge ribs, carbon tubes, carbon support and the wing skin. The geometrical modeling of the wing structural component was designed using Solidworks 2014 and the 3-dimensional model was imported to Abaqus software for numerical simulations. The wing was assumed to be symmetrical, therefore only half of the wing span model was used in the numerical analysis and lead to reduction in computation time. The materials used for the UAV wing was the Carbon fibre fabric (with Epoxy) and the Carbon fibre braided (with Epoxy) with various stacking sequence with the skin of the wing having a sequence of [0₂, 45, -45, 0_{1/2}]_s with 9 layers. The total thickness of the components would be 0.002286m. All of the components use the mesh generation which are Quad-Dominated and automatic structured meshing. The boundary condition 'Encaste' was applied at the fuselage-wing interface and the wing was subjected to wing loading of 8140.35N/m². The maximum deflection recorded was 1.780mm, which occurs at the wing tip. A high deflection means that it would disturb flight performance, thus reducing the battery management system of UAV ending with shorter range and endurance. The UAV wing has a Tsai-Hill value 0.1806 and Tsai-Wu value 0.1734. Both failure index showed that the UAV wing is much capable of handling the load acted upon it as both are less than 1 which brings meaning that they do not fail. In summary, researchers have used finite element analysis software Abaqus for structural analysis of UAV wing using carbon fibre of different fibre orientations and stacking sequence. The results were confirmed by experimental analysis. Abaqus software was used in this research for the structural analysis of an Unmanned Aerial Vehicle wing made from SterculiaSetigeraDelile fibre, PterocarpusErinacues Epoxy composite and structural analysis was used for the confirmation of the results [7].

2. Material and Method

2.1. Modeling of the UAV

The UAV wing parameters initially used in this simulation consist of 1 spars, 2 ribs, and 2 wing skin.

Table 1. Important parameters for the UAV wing

Parameters	Value
Span length, b (mm)	924
Chord length, c, (mm)	147
Aspect Ratio (A.R)	6.28
UAV weight(kg)	3
Number of spars	1
Number of ribs	2
Number of Wing Skin	2
Spar Height(mm)	15.40
Spar Thickness(mm)	2.5
Wing Skin Thickness(mm)	2
Spar thickness(mm)	2.5

The geometric modeling of the UAV wing was done using ABAQUS/CAE. The process involves airfoil selection in which high lift airfoil was selected. The airfoil selected was the Wortmann FX 63-137 (fx 63137-il) human power aircraft airfoil due to its high lift to drag ratio and high stall angle [8]. Only half span of the wing was modeled to reduce the number of elements and to reduce the computation time.

Finite Element Method was used to predict the structural response which becomes overly complex with calculations. The static structural analysis was performed using Finite Element Software ABAQUS /CAE. ABAQUS was chosen since it has pre-processing features that makes composite material property definition easier [4].

The UAV Wing was modeled as follows:

Part module- Abacus Software was used to model the components of the wing for simulation. The coordinates of the Airfoil were imported from the Airfoiltol website which was used in creating the Wing skin, Spars and wing ribs.

Material module- The mechanical properties were specified in the module, specifying the angle of orientation and the specified thickness. The software has a composite layup manager which allows the stacking of composites at specified angles of orientation and with varying thickness.

Assembly module- Assembly of the UAV wing.

Load module- ENCASTRE boundary condition was applied to the Root Rib connection to the fuselage which would prevent translation and rotation in all directions [4,7, 9]. The load distribution calculated using the Schrenk method was applied on the wing. The wing was divided into four sections and the pressure was applied to each section.

Meshing - The global seed mesh was generated for the whole model with an approximate size of 0.5mm. Quad-dominated shape element and structured mesh technique were used for the whole wing except for the ribs with many curved edges. The mesh technique used for the ribs was free mesh [4,9]. Tsai Hill and Tsai Wu's failure Criterion was to analyze the failure of the wing.

Job- The Job process was initiated and after completion, the failure was analyzed using the Tsai-Hill, Tsai-Wu failure criterion.

Table 2. Mechanical properties of composite materials used for the simulations [4, 10]

Mechanical Properties of optimum composite	Cold SSD 5% WD=7.5%	Woven Carbon fibre Epoxy
Tensile Strength Longitudinal(MPa)	26.90	600
Tensile Strength Transverse(MPa)	6.63	600
Flexural Strength (MPa)	77.38	-
Compression Strength Longitudinal direction(MPa)	53.25	570
Compression Strength Transverse Direction(MPa)	31.52	570
Poisson ratio, ν_{12}	0.41	0.1
Poisson ratio, ν_{23}	0.37	0.1
Elastic Modulus E_1 (GPa)	1.16	70
Elastic Modulus E_2 (GPa)	0.9	70
Shear Strength(MPa)	4.16	90
Shear Modulus, G_{12} (GPa)	0.411	5
Shear Modulus, G_{13} (GPa)	0.411	5
Shear Modulus, G_{23} (GPa)	0.33	5



Fig. 1 Modeled unmanned aerial vehicle wing using Abaqus software

The wing was subjected to various loadings under the regulations of Federal Aviation Regulation (FAR) part 23: Airworthiness Standard. The maximum load factor that was used was 3.8 which is the maximum wing loading that would be experienced during flight and a safety factor of 1.5 making it an ultimate load factor of 5.7 [11]. For a 3kg UAV, the ultimate load is calculated as follows:

$$L = nW \tag{1}$$

$$UL = 3 \times 9.81 \times 3.8 \times 1.5 = 167.75 N .$$

2.2. Calculation of Lift Distribution Using Schrenk Method

The Schrenk method is simple approximation methods of finding spanwise lift distribution which has been proposed by Dr. Ing Oster Schrenk and has been accepted by the Civil

Aeronautics Administration (CAA) as a satisfactory method for civil aircraft. Schrenk method uses the average between the planform lift and elliptical lift distribution. The mathematical model for the Schrenk method is shown [12]:

$$L'_{elliptical} = \frac{4L}{\pi b} \sqrt{1 - \left(\frac{2y}{b}\right)^2} \tag{2}$$

$$L'_{planform} = \frac{2L}{(1 + \lambda)b} \left(1 + \frac{2y}{b} (\lambda - 1)\right) \tag{3}$$

$$L'_{schrenk} = \frac{L'_{elliptical} + L'_{planform}}{2} \tag{4}$$

where L : total lift force (N), L' : lift distribution (N/m), λ : Taper ratio, b = wingspan (m) , y : spanwise distance of section(m) [12]. The formula is used in the calculation of the lift distribution on the wing.

The Schrenk method assumes that the lift distribution along the wingspan is the average lift based on the trapezoidal and the lift based on the elliptical wing. To determine the aircraft lift distribution, the wing was divided into 40 sections each having a span of 11.55mm.

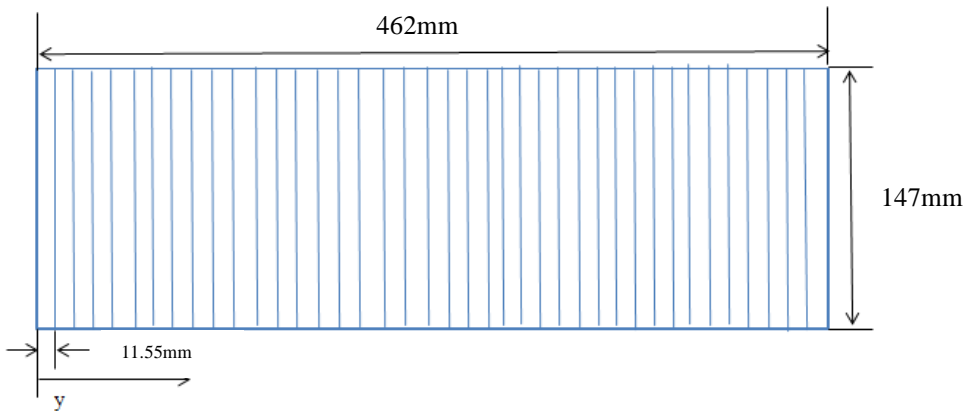


Fig. 2 Half span UAV wing divided into 40 sections for lift distribution calculation

For a 3kg UAV Wing, the Ultimate load was calculated as 167.75N. This was used for the estimation of the load distribution using the Schrenk method.

Trapezoidal Wing:

$$L(y) = \frac{2L}{b(1 + \lambda)} \left[1 - \frac{2y}{b} (1 - \lambda)\right] \tag{5}$$

Elliptical Lift:

$$L(y) = \frac{4L}{\pi b} \sqrt{1 - \left(\frac{2y}{b}\right)^2} \tag{6}$$

Trapezoidal Wing at $y=0$ $L(0) = \frac{2 \times 167.75}{0.924 \times (1+1)} \left[1 - \frac{2(0)}{0.924} (1-1) \right] = 181.55 \text{ N/m}$

Elliptical Lift at $y=0$, $L(0) = \frac{4 \times 167.75}{3.141592 \times 0.924} \sqrt{1 - \left(\frac{2 \times 0}{0.924}\right)^2} = 231.155 \text{ N/m}$

$$L'(0) = \frac{181.55 + 231.155}{2} = 206.353 \text{ N/m}$$

Trapezoidal Wing at $y = 0.01155\text{m}$,

$$L(0.01155) = \frac{2 \times 167.75}{0.924 \times (1+1)} \left[1 - \frac{2(0.01155)}{0.924} (1-1) \right]$$

$$= 181.55 \text{ N/m}$$

Elliptical Lift at $y=0.01155$, $L(0.01155) = \frac{4 \times 167.75}{3.141592 \times 0.924} \sqrt{1 - \left(\frac{2 \times 0.01155}{0.924}\right)^2}$
 $= 231.083 \text{ N/m}$

$$L'(0.01155) = \frac{181.55 + 231.083}{2} = 206.3165 \text{ N/m}$$

Where L is the Limit load; b is the span length of the wing; λ is the taper ratio; $L(y)$ is the lift distribution in N/m.

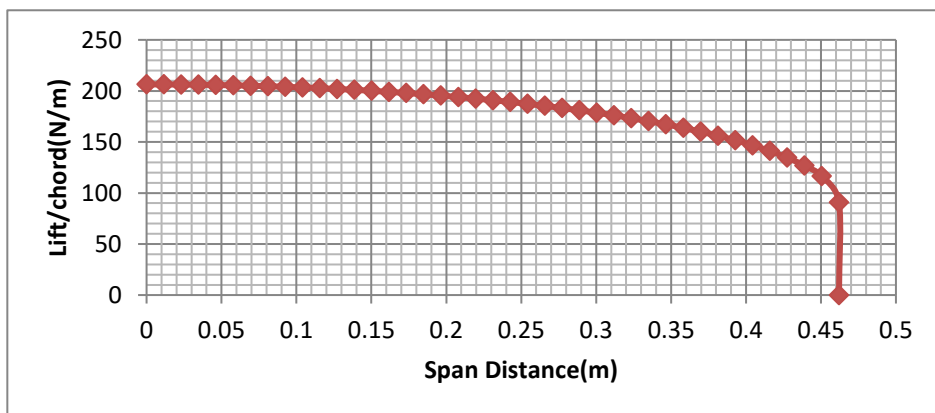


Fig. 3 Lift distribution over the half-span wing calculated using Schrenk method (3kg UAV)

2.3. Load and Boundary Conditions

The Load distribution across the wing span was estimated using the Schrenk method. The weight of the structure is automatically calculated by considering the material input into

ABAQUS pre-processing. ENCASTE boundary condition was applied to the root ribs which interfaces the fuselage. This would prevent rotation and translation in all direction. The wing tip is free from constraint in all degree of freedom. The overall loads and boundary conditions acting on the model are shown in figure 4:

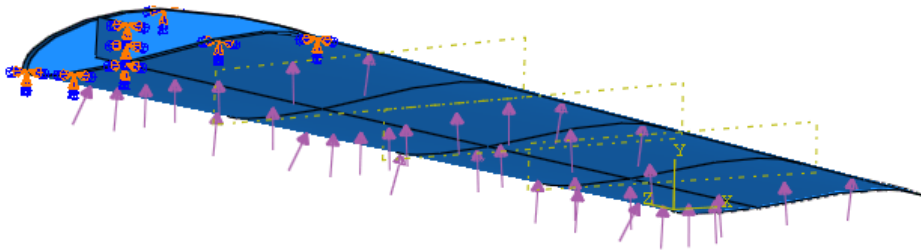


Fig. 4 ENCASTE boundary condition was applied to the root rib and the load pressure distribution applied to the lower wing region based on Schrenk method.

2.4. Meshing

Mesh Convergence study was conducted for a global size mesh of 5mm to 0.35mm. The global size of the mesh was chosen for the whole model with the size of approximately 0.5mm after the mesh convergence study [4]. The mesh control was activated for regulating the shape of the element and meshing technique. Quad-dominated shape element and free meshing technique was used. The ribs, contains many curved edges, the meshing technique used was free meshing technique and triangular element was used.

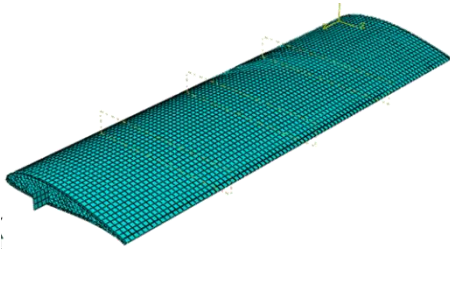


Fig. 5 Meshed result of the unmanned aerial vehicle wing for 5mm global size mesh

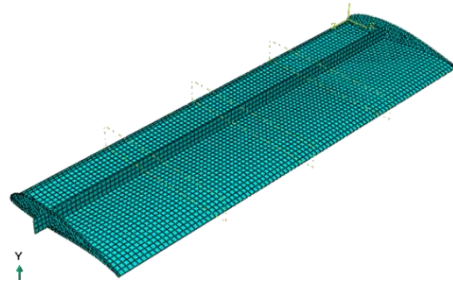


Fig. 6 Meshed result for the inner structure of the unmanned aerial vehicle wing for 5mm global size mesh

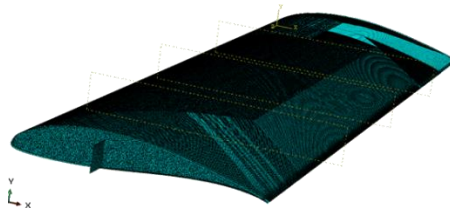


Fig. 7 Meshed result of the unmanned aerial vehicle wing for 0.5mm global size mesh

2.5 Composite Failure Theory Criterion

Failure Criterion is used to measure the ability of the structure to withstand a given load, whether it fails or not. The Tsai Hill and Tsai Wu failure criterion can be used to examine the failure of a composite material like the composite Unmanned Aerial Vehicle Wing.

2.5.1 Tsai Hill Failure Criterion

The Tsai-Hill failure criterion is based on distortion energy theory of Von Mises distortion energy yield criterion. The distortion energy is part of the strain energy of the body. The strain energy consists of two parts; the first part is as a result of change in volume of the body and it is known as the dilation energy and the second part of the strain energy is due to the change in shape of the body and is called distortion energy. The failure of the body occurs when the distortion energy is greater than the distortion energy of the material. Based on the distortion energy theory Tsai and Hill proposed that a lamina will fail if it does not satisfy Equation 7:

$$(G_2 + G_3)\sigma_1^2 + (G_1 + G_3)\sigma_2^2 + (G_1 + G_2)\sigma_3^2 - 2G_3\sigma_1\sigma_2 - 2G_2\sigma_1\sigma_3 - 2G_1\sigma_2\sigma_3 + 2G_4\tau_{23}^2 + 2G_5\tau_{13}^2 + 2G_6\tau_{12}^2 < 1 \quad (7)$$

is violated. Where:

$$G_1 = \frac{1}{2} \left[\frac{2}{[(\sigma_2^T)_{ult}]^2} - \frac{1}{[(\sigma_1^T)_{ult}]^2} \right] \quad (8)$$

$$G_2 = \frac{1}{2} \left(\frac{1}{[(\sigma_1^T)_{ult}]^2} \right) \quad (9)$$

$$G_3 = \frac{1}{2} \left(\frac{1}{[(\sigma_1^T)_{ult}]^2} \right) \quad (10)$$

$$G_6 = \frac{1}{2} \left(\frac{1}{[(\tau_{12})_{ult}]^2} \right) \quad (11)$$

Unidirectional lamina is assumed to be under plane stress, therefore $\sigma_3 = \tau_{13} = \tau_{23} = 0$

The equation reduces to [13, 14]:

$$\left[\frac{\sigma_1}{(\sigma_1^T)_{ult}} \right]^2 - \left[\frac{\sigma_1\sigma_2}{(\sigma_1^T)_{ult}^2} \right] + \left[\frac{\sigma_2}{(\sigma_2^T)_{ult}} \right]^2 + \left[\frac{\tau_{12}}{(\tau_{12})_{ult}} \right]^2 < 1 \quad (12)$$

Tsai-Hill theory considers the interaction among the three unidirectional lamina parameter. One of the drawbacks of the Tsai-Hill failure theory is that it does not distinguish between compressive and tensile strength in the equation. This can result to the underestimation of the maximum load that can be applied when compared to other failure theories. Tsai-Hill failure criterion can underestimate the failure stress of a component because the transverse strength of the unidirectional lamina is less than the transverse compressive strength.

2.5.2 Tsai Wu Failure Criterion

Tsai-Wu applied the failure criterion to a lamina in plane stress. A lamina is considered to fail if it does not satisfy the equation 13 [4,10]:

$$H_1\sigma_1 + H_2\sigma_2 + H_6\tau_{12} + H_{11}\sigma_1^2 + H_{22}\sigma_2^2 + H_{66}\tau_{12}^2 + 2H_{12}\sigma_1\sigma_2 < 1 \quad (13)$$

Tsai-Wu failure criterion is more general than the Tsai-Hill failure criterion because it distinguishes between the compressive strength and tensile strength of lamina. Where:

$$H_1 = \frac{1}{(\sigma_1^T)_{ult}} - \frac{1}{(\sigma_1^C)_{ult}} \tag{14}$$

$$H_{11} = \frac{1}{(\sigma_1^T)_{ult}(\sigma_1^C)_{ult}} \tag{15}$$

$$H_2 = \frac{1}{(\sigma_2^T)_{ult}} - \frac{1}{(\sigma_2^C)_{ult}} \tag{16}$$

$$H_6 = 0 \tag{17}$$

$$H_{66} = \frac{1}{(\tau_{12})_{ult}^2} \tag{18}$$

$$H_{12} = -\frac{1}{2(\sigma_1^T)_{ult}^2} \tag{19}$$

as per Tsai Hill failure theory [13,14].

Where $(\sigma_1^T)_{ult}$ is the tensile strength in fiber direction, $(\sigma_1^C)_{ult}$ is the compressive strength in the fibre direction, $(\sigma_2^T)_{ult}$ is the tensile strength in transverse direction, $(\sigma_2^C)_{ult}$ is the compressive strength in transverse direction, and $(\tau_{12})_{ult}$ is the shear strength.

2.6 Procedure for Loading of UAV Wing During Structural Test

The assembled UAV wing was subjected to structural test. Firstly, a gripping region was created at the root of the wing. The gripping region was created using the sisal fibre and the epoxy/hardener in order to simulate a fixed region. The gripping region acts as a holder during structural testing. The gripping region was used to ensure a fixed wing-fuselage interface region during testing. The Figure 8 shows the UAV wing being subjected to loading using sandbags and the deflection of wing being recorded using dial guage. The gripping region is shown in figure 9 and figure 10 shows the arrangement of the spar and ribs on the UAV wing skin. Figure 11 shows the fully assembled UAV wing. The UAV wing was inverted during testing since the wing loading is expected to be acting at the bottom of the wing. After gripping the UAV wing, the wing was divided into four equal sections. The UAV wing was subjected to wing loading as calculated using the Schrenk method for UAV of different masses. The deflection was recorded using a dial guage at the wing tip. The results were recorded and compared to simulation result.

The wing was subjected to various loadings under the regulations of Federal Aviation Regulation (FAR) part 23: Airworthiness Standard [8]. The limit load factor that was used was 3.8. It is used to find the maximum wing loading which would be experienced during flight and is multiplied with a safety factor of 1.5 to attain the ultimate load factor of 5.7. For a 3kg UAV the ultimate load is calculated as follows: . The UAV wing is divided into four sections using Schrenk method. The distributed load is divided into four sections: Section 1: 23.72/9.81=2.42kg; Section 2 = 22.78/9.81= 2.32kg; Section 3: 20.56/9.81 =2.10kg; Section 4: 15.74/9.81=1.61kg. The Ultimate load was divided by 2 since the simulated wing and tested was a half span [12, 13].

For a 3.5kg UAV the ultimate load was calculated as follows: . The distributed load was divided into four sections: Section 1: 27.63/9.81=2.82kg; Section 2: 26.54/9.81= 2.71kg; Section 3: 23.95/9.81 =2.44kg; Section 4: 18.334/9.81 =1.87kg. Refer to Table 4.



Figure 8 UAV wing subjected to loading using sandbags to determine its structural strength at the mechanical workshop, Bayero University Kano.



Figure 9 Fixture made from Sisal fibres and Epoxy Matrix attached to the root of the UAV wing to simulate the fuselage wing interface



Figure 10 Placement of the Spar on the wing skin and image of the ribs



Figure 11 Complete Unmanned Aerial Vehicle Wing

3. Result and Discussion

3.1 Performance Evaluation of UAV Wing Using Abacus Finite Element Method Software

Tsai Hill and Tsai Wu's failure criterion was used to analyze the failure of the UAV wing using Abacus FEM software. The Mechanical Properties used for Finite element Analysis includes Young's Modulus: E1, E2, Poissons Ratio: ν_{12} , Shear Modulus: G12, G13 and G23. Furthermore, other Strength parameters needed for the Tsai-Hill and Tsai-Wu failure criterion includes Longitudinal Tensile Strength , Longitudinal compressive Strength , Transverse Tensile Strength and Transverse Compressive Strength , in-plane shear strength and density(ρ). The section shows the images of the simulations results conducted for the UAV wing while subjecting the wing to various loading. The wing loading is based on the total mass of the UAV multiplied by ultimate load factor of 5.7 and acceleration due to gravity 9.81m/s². The factor is based on Federal Aviation regulation [11].

Mesh convergence studies was performed using h-refinement by reducing the size of elements to find the point at which the solution converges. The mesh convergence study graph is shown in figure 12. The Ultimate load used for the mesh convergence study was 167.5N (3kg). The result from the mesh convergence study is shown in Table 3. The result shows that as the number of element changes there is a significant change in the Tsai Hill, Tsai Wu failure criterion and the deflection of the UAV wing. Initially, a Global seed mesh size of 5mm was used to attain a Tsai Hill Value of 0.1274, as the mesh size was reduced to 4mm, the Tsai Hill value attained was 0.1335. The Tsai Hill value increased by a percentage of 4.79% from the 5mm size to 4mm. For the Global seed mesh from 0.5mm to 0.4mm. The Tsai Hill value increased by a percentage of 2.24%. The result showed a minimum increase in percentage difference as a result of increasing number of elements. A global seed mesh of 0.5mm was chosen for other simulations. The Element type chosen was the S3R S4R. The number of elements used for the simulations are 627574 and the no of nodes used are 606365.

S3R- 3-node triangular general-purpose or conventional shell/displacement shell with reduced integration and finite membrane strains. The nodes have six degree of freedom.

S4R is a 4-node quadrilateral, stress/displacement shell element, reduced integration with hourglass control and a large-strain formulation. The nodes have six degree of freedom [9].

Table 3. Mesh convergence study of the UAV wing

Value (Tsai Hill)	Tsai Wu	Deflection(mm)	No of Nodes	Number of Elements	Global Seed(mm)
0.1274	0.1319	4.846	6354	6644	5
0.1335	0.1382	4.834	9678	10100	4
0.1415	0.1465	4.826	17382	18055	3
0.1628	0.1700	4.817	151457	156861	1
0.1701	0.1780	4.816	269500	278638	0.75
0.1782	0.1872	4.815	606365	627574	0.50
0.1822	0.1918	4.815	945663	978263	0.4
0.1850	0.1949	4.815	1236069	1278832	0.35

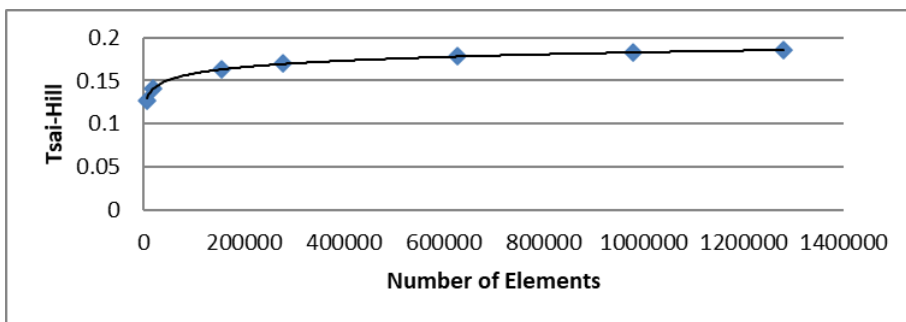


Fig. 12 Mesh convergence study of the UAV wing

The simulations results show the UAV wing response to wing loading. Tsai Hill, Tsai Wu failure criterion and deflections of the UAV wing is used to analyze the failure response of the wing.

The Figure 13-15 shows the Tsai Hill, Tsai Wu failure criterion value and the deflection of the UAV wing. The result in figure 13 shows that when a load of 167.75N (3kg UAV) is applied to the UAV wings the wing has a Tsai Hill failure value of 0.1767, Tsai Wu value of 0.1856 and a maximum wing deflection of 4.757mm. The Tsai Hill and Tsai Wu failure values are both less than 1 meaning that it satisfies their failure criterion.

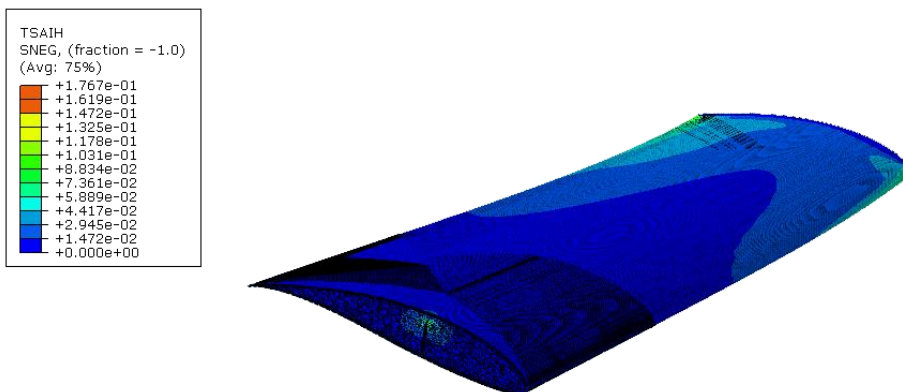


Fig. 13 Failure analyses of 3kg UAV (Tsai Hill)

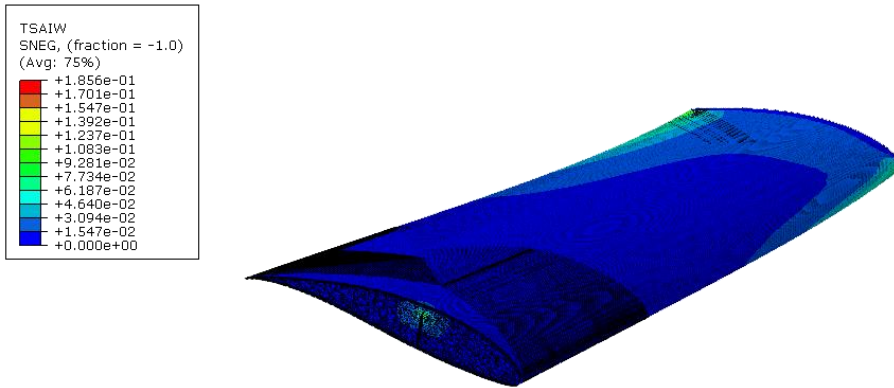


Fig. 14 Failure analyses of 3kg UAV (Tsai Hill)

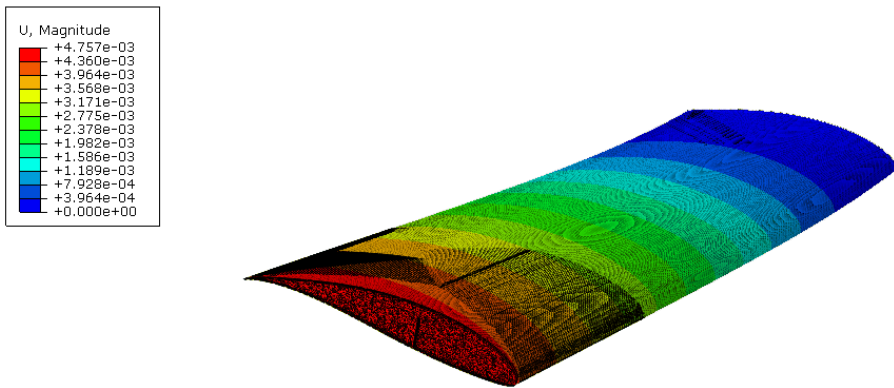


Fig. 15 Deflection of 3 kg unmanned aerial vehicle wing in meters

For figure 16-18, the load applied for a 4.5kg UAV wing was 251.63N distributed over both wings. Since half span of the wing was subjected to the simulation, half of the load was distributed over the wing. The result showed that after subjecting the UAV wing to wing loading, the wing had a Tsai Hill, Tsai Wu and deflection value of 0.265, 0.2784 and 7.135mm respectively. The Tsai Hill and Tsai Wu value satisfies their failure criterions because both values are less than 1.

For figure 19-21, the load applied for a 16kg UAV wing was 895N distributed over both wings. The result showed that after subjecting the UAV wing to wing loading, the wing had a Tsai Hill, Tsai Wu and deflection value of 0.9422, 0.9899 and 25.37mm respectively. The Tsai Hill and Tsai Wu value satisfies their failure criterions because both values are less than 1. Simulation was also performed using Carbon fibre epoxy as the material for the UAV wing. The UAV wing was subjected to wing loading of 167.5N to 951N. The Tsai Hill value was between 0.004667 to 0.02644 respectively and the Tsai Wu value was between 0.004740-0.0266 respectively for a wing loading of 167.5N to 951N. The deflection of the UAV wing was between 0.09576mm to 0.5427mm respectively. The results clearly showed that Carbon fibre epoxy composite has higher resistance to failure and higher resistance to deflection. The result of the Carbon fibre epoxy wing analysis is shown in table 6. At the wing loading of 895N, the SterculiaSetigeraDelile fibre- PterocarpusErinaceus epoxy composite wing had a Tsai-Hill value (0.9425), Tsai-Wu (0.9902) and deflection

(25.37mm) for deflection while for the Carbon fibre epoxy composite wing had a Tsai-Hill value (0.0249), Tsai-Wu (0.02528) and deflection (0.5107mm) respectively.

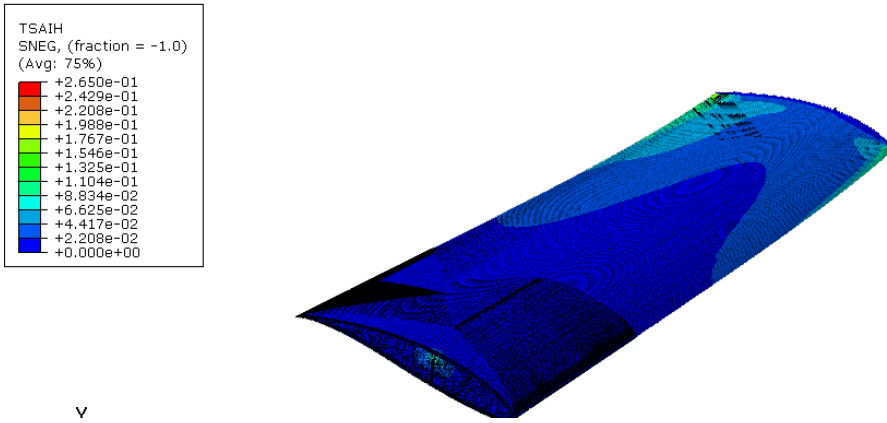


Fig. 16 Failure analyses of 4.5 kg UAV (Tsai Hill).

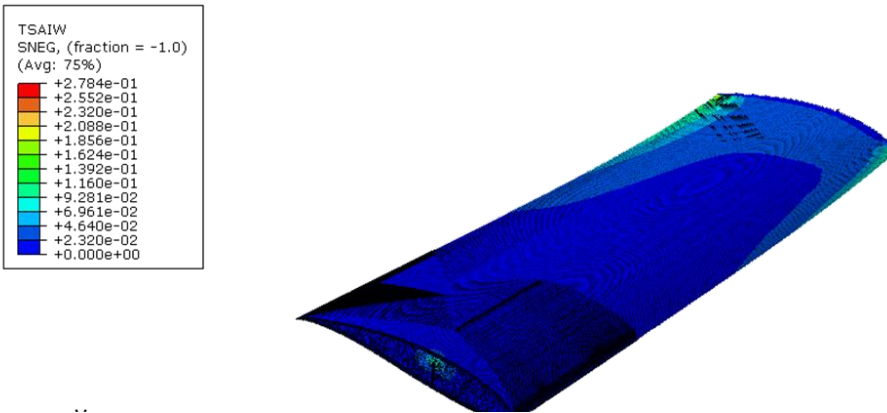


Fig. 17 Failure analyses of 4.5 kg UAV (Tsai Wu)

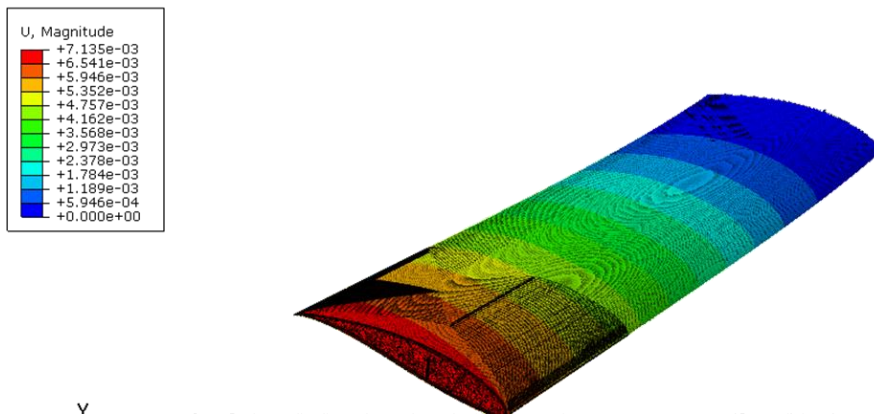


Fig. 18 Deflection of 4.5 kg unmanned aerial vehicle in meters

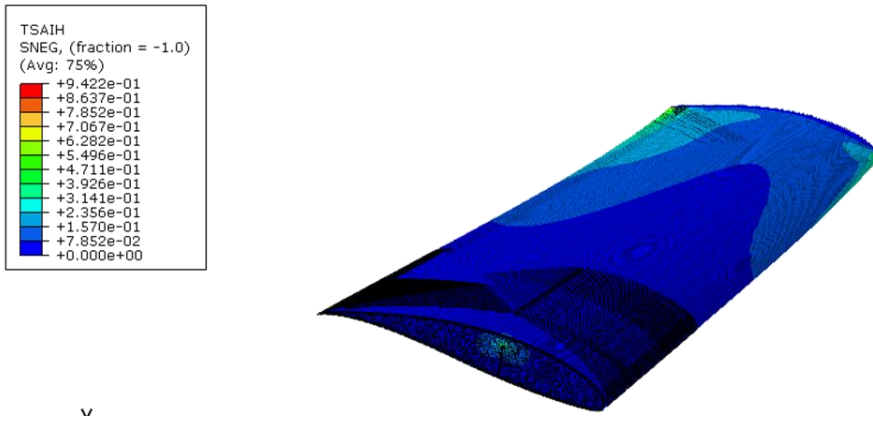


Fig. 19 Failure analyses of 16kg UAV (Tsai Hill)

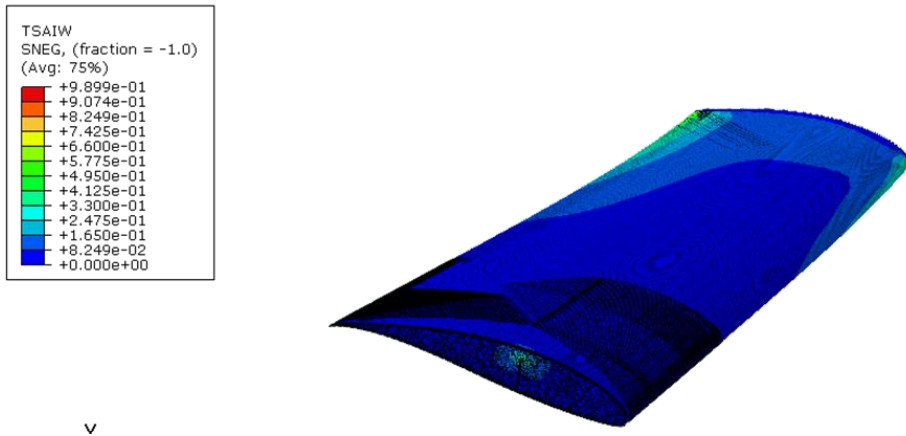


Fig. 20 Failure analyses of 16kg UAV (Tsai Wu)

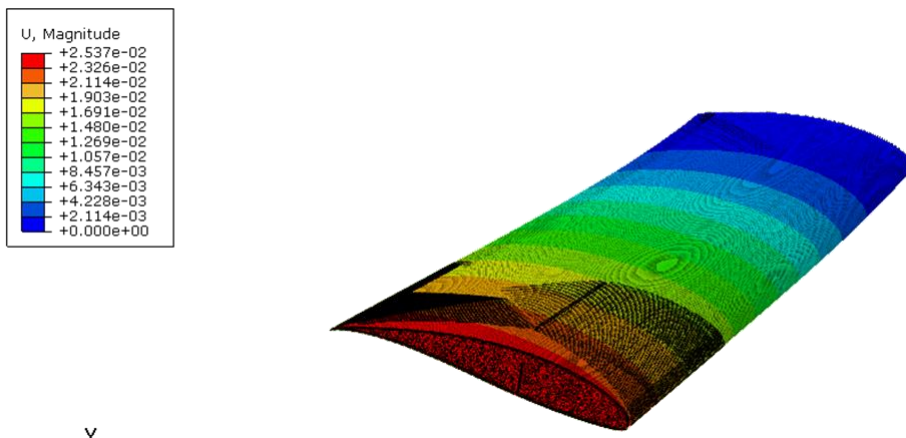


Fig. 21 Deflection of 16 kg unmanned aerial vehicle in meters

3.2 Structural Testing of the Unmanned Aerial Vehicle Wing

Structural test was performed on the wing with a wing loading from 167.75 to 335.50N (3 to 6kg UAV). The result shows the maximum deflection of the Unmanned Aerial Vehicle wing when subjected to wing loading using sand bag is shown in Table 4. The results were compared to result obtained from simulation using Abaqus Simulia software. The result showed that the UAV wing could withstand a wing loading of 335.50N (6kg).

Table 4. Loads placed in different sections of the UAV wing and its deflections

Ultimate load(N)	Section 1(kg)	Section 2(kg)	Section 3(kg)	Section 4 (kg)	Maximum Deflection at wingtip(mm)	
					Simulation Result	Experimental Result
167.5(3kg)	2.42	2.322	2.10	1.61	4.757	5
195.71 (3.5kg)	2.82	2.71	2.44	1.87	5.550	6
223.668 (4kg)	3.224	3.10	2.80	2.14	6.342	8
251.63 (4.5kg)	3.63	3.48	3.14	2.40	7.135	10
279.585 (5.0kg)	4.024	3.86	3.49	2.67	7.935	11
335.502 (6.0kg)	4.83	4.64	4.186	3.20	9.519	13

Table 5. Tsai-Hill, Tsai-Wu failure criterion and deflection of UAV wing

Ultimate load(N)	Tsai Hill failure index	Tsai Wu failure index	Maximum Deflection at wingtip (mm)		% Difference between Experimental and Simulation Deflection
			Simulation Result	Experimental Result	
167.5 (3kg)	0.1767	0.1856	4.757	5	5.11
195.71 (3.5kg)	0.2061	0.2166	5.550	6	8.10
223.668N (4kg)	0.2356	0.2475	6.342	8	26.14
251.63(4.5 kg)	0.2650	0.2784	7.135	10	40.15
279.585 (5.0kg)	0.2947	0.3096	7.935	11	38.63
335.502 (6.0kg)	0.3535	0.3714	9.519	13	36.57
447.336 (8.0kg)	0.4711	0.4950	12.69	-	-
559.17 (10kg)	0.5893	0.6191	15.87	-	-
726.921 (13kg)	0.7656	0.8043	20.61	-	-
838.755 (15kg)	0.8838	0.9286	23.80	-	-
895 (16kg)	0.9425	0.9902	25.37	-	-
951 (17kg)	1.002	1.053	26.98	-	-

The Ultimate load the wing can withstand from Table 5 was 895N based on the TsaiHill and Tsai Wu failure Index. In order to find the Ultimate load factor, for a 4.5kg UAV the Ultimate load factor was found using:

$$UL=nW$$

$$895=n \times 4.5 \times 9.81$$

$$n=20.27$$

Table 6. Tsai-Hill, Tsai-Wu failure criterion and Deflection of UAV wing for woven carbon fibre epoxy

Ultimate load(N)	Tsai Hill failure index	Tsai Wu failure index	Maximum Deflection at wingtip (mm)
			Simulation Result for woven carbon fibre epoxy material
167.5 (3kg)	0.004667	0.004740	0.09576
195.71 (3.5kg)	0.005445	0.005530	0.1117
223.668N (4kg)	0.006222	0.006320	0.1277
251.63 (4.5kg)	0.007000	0.007110	0.1436
279.585 (5.0kg)	0.007778	0.007900	0.1596
335.502 (6.0kg)	0.009333	0.009479	0.1915
447.336 (8.0kg)	0.01244	0.01264	0.2544
559.17 (10kg)	0.01556	0.01580	0.3192
726.921 (13kg)	0.02022	0.2054	0.4150
838.755 (15kg)	0.02333	0.02370	0.4788
895 (16kg)	0.0249	0.02528	0.5107
951 (17kg)	0.02644	0.02686	0.5427

3.3 Comparison Between Simulation and Experimental Testing of the UAV Wing

The material selected for the composite UAV wing was the Cold SSD 5% PTE wood dust 7.5% at 0-degree orientation. The UAV wing performance was simulated using the ABACUS software with various wing loadings on the wing. In this research Tsai Hill and Tsai Wu failure criteria were used to examine the ability of the optimum composite material to withstand load [15]. The results from Table 5 have shown that the UAV wing produced satisfies the Tsai-Hill and Tsai Wu failure criterion of being less than 1. Simulation result shows that the UAV wing could withstand a wing loading from 167.75N to 895N. Structural test was performed on the wing with a wing loading from 167.75 to 335.50N (3 to 6kg UAV). The UAV wing successfully resisted the loading. However, for the wing tip deflection there was a variation between 5.11%-40% between the maximum wing deflection simulations to the experimental result. The result showed that the wing could withstand the most critical flight load distribution in conformation with the Federal Aviation Regulation (FAR) part 23 Airworthiness for a normal category general aviation airplane with an Ultimate design load factor of 5.7. At the point of failure the wing could withstand

an Ultimate load factor of 20.27 which is 255.6% higher than the prescribed Ultimate design load factor of 5.7. This means that the UAV wing can withstand a load factor that is 255.6% higher than the prescribed ultimate load factor 5.7. For good comparison between the simulation and experimental result, the UAV manufacturer needs to ensure good bonding at the interface between the wing and the fuselage which is the key to good wing performance [5, 7].

3.4 Comparison Between Carbon Fibre Epoxy Composite and SSD fibre/PTE Wood Dust Epoxy Composite Wing

For the Carbon fibre epoxy composite UAV wing an Ultimate load of 251.63N(4.5kg mass UAV) was applied to the wing, the maximum wing deflection recorded from the Abaqus simulation result was 0.1436mm as shown in table 6 while result for the SSD fibre/PTE wood dust epoxy composite wing simulation the recorded result was 7.135mm. There is a percentage difference of 98% in the maximum deflection between the two materials. The carbon fibre has greater resistance to deflection. For Carbon fibre epoxy composite an Ultimate load of 895N (16kg mass UAV) was applied to the UAV wing, the maximum deflection recorded from the Abaqus simulation result was 0.5107mm while result for the SSD fibre/PTE wood dust epoxy composite wing simulation the recorded result was 25.37mm. There is a percentage difference of 98% in the maximum deflection between the two materials. The carbon fibre has greater resistance to deflection. The carbon fibre epoxy composite UAV wing as expected has higher resistance to wing deflection. However, both the materials can withstand the wing loading requirement of the Federal Aviation Regulation. The advantages of SSD fibre/PTE wood dust epoxy composite when compared to the carbon-epoxy material is that the material is renewable, environmentally friendly, less pollution in the production of material and lower cost. The SSD fibre/PTE wood dust performance could be improved by optimization techniques.

4. Conclusion

In this research a 3 dimensional model of UAV wing was drawn, assembled and simulated using Abaqus software. The simulation results showed that the UAV wing could withstand a wing loading of 167.75 to 895N (3kg to 16kg UAV) meaning an Ultimate load factor of 20.27. This means that it could withstand an Ultimate load factor of 20.27 for a UAV with a 4.5kg mass. The Ultimate load factor of the wing was found by dividing the Ultimate load the Wing could withstand which was 895N by the UAV weight of 4.5kg multiplied by the acceleration due to gravity. The ultimate load factor given by the Federal Aviation Regulation was 5.7 meaning that the UAV wing should be able to withstand an ultimate load factor of 5.7. The 167.75 to 895N are the forces distributed incrementally on the UAV wing to analyze whether the wing could withstand the Ultimate load factor given by the Federal Aviation Regulation. The result means that components of higher weight such as weaponry and standard high quality cameras could be attached to the UAV. The UAV wing was successfully manufactured and structurally tested to validate the results from the simulation. The UAV wing was subjected to wing loading 167.75N to 335.50N (3kg to 6kg UAV mass). The UAV wing was able to withstand the pressure applied using sandbags successfully. The distribution of pressure was found using Schrenk method. In summary light weight Unmanned Aerial Vehicle wing was successfully produced using Wood fibre and wood dust epoxy composite and it was able to withstand the estimated wing loading. The composite produced has the potential to be used in the Aerospace industry due to its low density. Weight is an important factor in the aerospace industry as it affects the fuel consumption of aerospace vehicles. Furthermore, the production of synthetic fibres for composites has a negative impact on the environment. The use of natural fibre hybrid composite provides locally available wood fibres and wood dust for potential production of the Unmanned Aerial vehicles.

References

- [1] Warsi FA, Hazry D, Ahmed FS, Joyo M K, Tanveer MH, Kamarudin H. Yaw, Pitch and Roll controller design for fixed-wing UAV under uncertainty and perturbed condition. IEEE 10th International Colloquium On Signal Processing and its Applications. Kuala Lumpur, 2014. <https://doi.org/10.1109/CSPA.2014.6805738>
- [2] Rana S, Figueiro R. Advanced Composite Material for Aerospace Engineering: Processing Properties and Applications., Duxford, United Kingdom, Wood head Publishing, 2016. <https://doi.org/10.1016/B978-0-08-100037-3.00001-8>
- [3] Hsu TR. Applied Engineering Analysis, New Jersey, USA, John Wiley and Sons Ltd, 2018.
- [4] Rumayshah K, Prayoga A, Moelyadi MA. Design of High Altitude Long Endurance UAV: Structural Analysis of Composite Wing using Finite Element Method. IOP Conference Series: Journal of Physics: Conference Series 1005. IOP Publishing, 2018. <https://doi.org/10.1088/1742-6596/1005/1/012025>
- [5] Sullivan R, Hwang Y, Rais-Rohani M, Lacy T. Structural Analysis and Testing of an Ultralight Unmanned-Aerial-Vehicle Carbon-Composite Wing. Journal of Aircraft, 2009; 46(3): 814-820. <https://doi.org/10.2514/1.36415>
- [6] Kanesan G, Mansor S, Abdul-Latif A. Validation of UAV Wing Structural Model for Finite Element Analysis. Jurnal Teknologi, 2014; 71(2): 1-5. <https://doi.org/10.11113/jt.v71.3710>
- [7] Hutagalung MA, Latif AA, Israr HA. Structural Design Of UAV Semi-Monoque Composite Wing. Journal of Transport System Engineering, 2016; 3(1): 26-34.
- [8] Airfoiltools. WORTMANN FX 63-137 AIRFOIL (fx63137-il) Xfoil prediction polar at RE=200,000 Ncrit=9. [Internet]. Airfoiltools; 2021, Available from <http://airfoiltools.com/polar/details?polar=xf-fx63137-il-200000>
- [9] Dassault Systems. Abaqus 6.11: Abaqus/CAE User's Manual. Rhode Island: Dassault Systems, 2011.
- [10] Tahir NM, Alhaji AU and Abdullahi I. (In press). Optimization Of Mechanical Properties Of Hybrid Biocomposite From Sterculia Setigera Delile Fibre And Pterocarpus Erinaceus Wood Dust Epoxy. Wood Industry and Engineering.
- [11] Federal Aviation Administration. User's Guide for FAR23 Loads Program [Internet]. Federal Aviation Administration; 1997. Available from: <http://www.tc.faa.gov/its/worldpac/techrpt/ar96-46.pdf>
- [12] Soemaryanto A, Rosid N. Verification Of Schrenk Method For Wing Loading Analysis Of Small Unmanned Aircraft Using Navierstokes Based Cfd Simulation. Jurnal Teknologi Dirgantara, 2018; 15(2): 161-166. <https://doi.org/10.30536/j.jtd.2017.v15.a2747>
- [13] Kaw A. Mechanics of composite materials, 2nd edition, Florida, U.S.A, Taylor and Francis, 2006. <https://doi.org/10.1201/9781420058291>
- [14] Kolios AJ, Proia S. Evaluation of the Reliability Performance of Failure Criteria for Composite Structures. World Journal of Mechanics, 2012; 5: 162-170. <https://doi.org/10.4236/wjm.2012.23019>
- [15] Rajanish M, Nanjundaradhya NV, Sharma RS and Bhaskar PA. Review Of Failure Of Composite Materials. International Journal of Engineering Research and Applications (IJERA), 2013; 3(2):122-124.